

REVIEW

Open Access



# *Calotropis gigantea* assisted green synthesis of nanomaterials and their applications: a review

Shriniwas P. Patil

## Abstract

**Background:** Nanotechnology has been receiving wonderful impetus in the current emerging technological era by opening a pool of scientific ideas to compete with the daily challenges of developing technology. So far, numerous properties and countless applications of nanomaterials have been explored which have been even proved to be based on characteristic shape, size, surface area and surface chemistry.

**Main content:** By the time, several attempts have been made for green synthesis of nanomaterials, using plant extracts. *Calotropis gigantea* (L.) R. Br is the plant belonging to Apocynaceae, have been screened and proved to possess various pharmacological activities, due to different polar phytochemicals like flavonoids, lignans and terpenoids. This review focus on phytochemicals so far reported from different parts of the plant; pharmacological activities exhibited; green synthesis of nanomaterials, particularly metallic nanoparticles green synthesised by facilitating reaction of metallic ion donor molecule/salt and aqueous extract of leaves or flowers of *C. gigantea* and their biological or non-biological applications. The use of *C. gigantea* in the fabrication of nanomaterials is an eco-friendly and safe approach. Secondary metabolites present act as a stabilizing agent for nanomaterials. Cadmium sulphide, titanium dioxide, nickel and nickel oxide nanoparticles synthesised using *C. gigantea* exerted better anti-microbial action, compared to extracts. Nanoencapsulated magnesium oxide nanoparticles avoided biochemical degradation of MgO; increase its bioavailability and proved beneficial in type II diabetes mellitus. Cupric oxide nanoparticles got applied in dye-sensitised solar cell. Silver nanoparticles showed better cytotoxicity in HeLa cells. Biomaterial-supported zero-valent iron and stannic oxide nanoparticles proved to have utilities in water purification. Green synthesised  $\text{Eu}^{3+}$  doped  $\text{Y}_2\text{SiO}_5$  nanophosphors had significant chromaticity coordinates and average correlated colour temperature, hence find application in displays.

**Conclusion:** Variety of nanomaterials including nanoparticles and nanophosphors could successfully be biosynthesised using *Calotropis gigantea* extract or its latex. These green synthesised nanomaterials have several applications in the healthcare system and technology.

**Keywords:** Nanotechnology, *Calotropis gigantea*, Metal nanoparticles, Zero-valent iron nanoparticles,  $\text{Eu}^{3+}$  doped  $\text{Y}_2\text{SiO}_5$  nanophosphors, Applications

Correspondence: [patilsp111@gmail.com](mailto:patilsp111@gmail.com)

Department of Pharmacognosy, SCES's Indira College of Pharmacy, Pune 411 038, India

## 1 Background

Nanotechnology has gained marvellous impetus in today's rapidly emerging technological era by generating a wealth of scientific concepts to tackle with daily challenges of developing technology [1]. The nanomaterials have been proved to possess countless applications and physico-chemical properties [2, 3] which are exerted due to their characteristic size, shape, area and surface chemistry [4]. These features of nanomaterials enable them to be highly reactive and thereby more attractive for researchers [5]. These nanomaterials may exist in the form of nanotubes, nanocrystals, nanoparticles, nanospheres, nanophosphors or even in their combination, i.e. nanohybrids. In the recent era, different metallic nanoparticles are gaining research interest in material chemistry due to their unique catalytic, electrical and optical characteristics. These nanomaterials could be conjugated with various functional biomolecules such as antibodies, ligands, and drugs of interest for biomedical applications.

### 1.1 Manufacturing of nanomaterials

Depending upon the particular type, nanomaterials can be manufactured by one of the two approaches: *bottom-up* and *top-down*. The bottom-up approach involves placing of atom by atom or molecule by molecule; which can be achieved by chemical synthesis, self-assembly and positional assembly. Top-down strategy implicates etching, milling or grinding of a larger piece of material to be converted to its nanoform. In this approach, complex devices are used, requiring high energies and producing more wastes. Hence, bottom-up strategies are preferred where atoms or molecules are get arrange themselves into ordered nano-structures by physical and/or chemical interactions.

## 2 Main text

As far as *Calotropis gigantea* is concerned, different research articles pertaining to a variety of aspects, right from primary microscopic features of different parts, their preliminary phytochemical evaluation, various pharmacological screening and application of its extracts in green synthesis of nanomaterials have been published. Most of these research articles are available on internationally reputed, well-recognised search engines like ScienceDirect (<http://www.sciencedirect.com>), Wiley Online Library (<http://onlinelibrary.wiley.com>), Springer (<http://link.springer.com>), Taylor and Francis (<http://www.tandfonline.com>), Nature ([www.nature.com](http://www.nature.com)) and PubMed (<http://www.ncbi.nlm.nih.gov/pubmed>). This review highlighted the phytochemicals reported to be present in a given part of plant *Calotropis gigantea* which could be claimed to be present in extract using which several successful attempts of green synthesis of nanomaterials were made. This review throws the light on the method used for their green synthesis as well as the

biological/pharmacological and non-biological applications of these nanomaterials.

### 2.1 Botanical description of *Calotropis gigantea*

The word *Calotropis* was derived from the Greek word "*Kalos*" meaning beautiful and "*tropis*" meaning keel, referring to the shape of the coronal scales. *Calotropis gigantea* (crown flower) (Fig. 1) is a large shrub or small tree, belonging to family Asclepiadeae, characterised by the presence of a smooth and soft tomentum on stems and lower leaf surfaces, calyx lobes with many glands at the base, broadly campanulate corollas, and coronal scales with a recurved spur at the base. Among various species, this one, *C. gigantea* is an Asiatic, occurring widely throughout the Indian subcontinent, southern China, South East Asia and has also been introduced into New Guinea and Hawaiian islands [6].

### 2.2 Phytochemical composition of *Calotropis gigantea*

Over time, variety of secondary metabolites have been reported to be isolated from different parts of *Calotropis gigantea* and structurally elucidated.

As per Lhinhatrakool T, Sutthivaiyakit S. [7], the leaves of *C. gigantea* contain pinosresinol, medioresinol, uzarigenin, calotropin, calactin, calacitnic acid, calacitnic acid methyl ester, 19-carboxyl-calacitnic methyl ester, drummondol, 15b-hydroxycalotrin, the C-11 bicyclic lactone, norisopenoid, the rare diphenyl furfuran lignan and



**Fig. 1** *Calotropis gigantea* (Crown flower), belonging to family Asclepiadeae

salicifoliol. Seeka and Sutthivaiyakit [8] isolated 15- $\beta$ -Hydroxycardenolides and 16- $\alpha$ -hydroxycalactinic acid methyl ester while Nguyen et al. [9] isolated a lignan, 9'-methoxypinoresinol and two new glycosylated 5-hydroxymethylfurfurals, calofurfuralside A and calofurfuralside B from the leaves of *C. gigantea*. Di-(2-ethylhexyl) Phthalate and anhydrosophoradiol-3-acetate were isolated from flower [10]. Sen et al. [11] isolated flavonol glycosides, isorhamnetin-3-O-[2-O- $\beta$ -D-galactopyranosyl-6-O- $\alpha$ -L-rhamnopyranosyl]- $\beta$ -D-glucopyranoside, isorhamnetin-3-O-rutinoside, isorhamnetin-3-O-glucopyranoside and taraxasteryl acetate from aerial parts of *C. gigantea*. The fixed oil separated from seeds of *C. gigantea* was reported to contain lauric acid, myristic acid, palmitic acid, palmitoleic acid, stearic acid, oleic acid, linoleic acid, linolenic acid, arachidic acid and behenic acid (book chapter). These fatty acids are also present in the form of mono-, di-, and tri-acyl glycerols at the surface of and internal to leaves [12]. Terpenoids derivatives like pentacyclic Triterpenic Esters and lupeoul acetate were isolated from the roots of *C. gigantea* [13].

### 2.3 Pharmacological potential of *Calotropis gigantea*

*Calotropis gigantea* is a notorious weed, so far not cultivated commercially. Still, the plant has been screened for different pharmacological activities, in the form of extract of any part, isolated compound or latex, using

different scientifically accepted in-vivo or in-vitro models [14]. Based on phytochemicals present, different parts of *Calotropis gigantea* were reported to possess different pharmacological activities (Table 1).

### 2.4 Green synthesis of nano-structures and their applications

Several researchers tested the hypothesis which was based on nanostructures if synthesised using *C. gigantea* or its latex, could have improvement in pharmacological potential exhibited by different extracts prepared using different parts of *C. gigantea* or latex collected; or else, these nanomaterials could be used in non-biological applications like those in the field of energy or television displays (LEDs and LCDs).

### 2.5 Cadmium sulphide nanoparticles

In 2017, Ayodhya and Veerabhadram [29] synthesised cadmium sulphide nanoparticles using aqueous extract of leaves of *C. gigantea*. The extract was further mixed with 40 mL of 1 mM of cadmium acetate and 40 mL of 1 mM of sodium sulphide to obtain spherical CdS NPs. CdS NPs were then characterised for their morphology, stability and particle size; photocatalytic activity was studied under sunlight irradiation using MB and EY dyes. The XRD pattern of CDs NPs exhibited three prominent peaks at  $2\theta$  values of 26.4°, 43.4° and 51.6°;

**Table 1** Pharmacological activities of *C.gigantea*

Part of plant	Pharmacological Activity	Pharmacological model used	Reference
Flowers	Analgesic	Acetic acid induced writhing	[15]
Flowers	Anti-tumoric	Ehrlich's ascites carcinoma in mice	[16]
Latex	Antibacterial	Agar well diffusion method using cariogenic bacteria	[17]
Leaves	Antibacterial	Agar well diffusion method using Klebsiella spp	[18]
Flowers	Anti-fungal	Disc diffusion assay method using <i>Aspergillus flavus</i> and <i>Aspergillus fumigatus</i>	[10]
Flowers	Cytotoxicity	Brine shrimp lethality bioassay	
Aerial parts	Antipyretic	TAB (typhoid) vaccine-induced pyrexia in rabbits and Brewer's yeast-induced pyrexia in rats	[19]
Root bark	Antitumour	Ehrlich's ascites carcinoma in mice	[20]
Peeled roots	Anticonvulsant and skeletal muscle relaxant activity	Pentobarbitone-induced sleeping time model and rotating rod model	[21]
Leaves	Anticonvulsant and skeletal muscle relaxant activity	Maximal electroshock seizure (MES) and Strychnine-induced convulsions models and rotating rod model	[22]
Leaves	Cytostatic and cytotoxic activity	SRB assay using tumour cell lines: MDA-MB-231 (human breast cancer), PC-3 (human prostate cancer), MCF7 (human breast cancer), HT-29 (human colon cancer), 4 T1 (mouse mammary cancer), and RAW-267 (mouse leukemic monocyte macrophage)	[23]
Leaves	Antiplasmodial	Lactate dehydrogenase assay using human blood	[24]
Latex and fruits	HIF-1 inhibitory activities	T47D cell-based dual-luciferase reporter assay	[25]
Root bark	Wound healing	Excision, incision and dead space wound models	[26]
Roots	Pregnancy interception	Postcoital contraceptive efficacy evaluation	[27]
Latex	Procoagulant activity	Re-calcification time and fibrinolytic activity	[28]

corresponding to the (111), (220) and (311) diffraction planes of cubic crystals. The average particle size of CdS NPs was found to be 12 nm. The nanophase and quantum confinement nature of the synthesised CdS NPs was indicated by enhancement of the optical band gap of 2.42 eV. It was also observed that as in particle size decreases, the energy of separation between the ground and excited electronic states increases; resulting in a blue shift in absorption. The capping effects and functional groups of *C. gigantea* leaf extract phytochemicals on CdS NPs surfaces were investigated by ATR-FTIR. The longevity of CdS NPs was tested by recycling the photocatalyst used in the photocatalytic degradation of MB and EY dyes under 60 min of sunlight irradiation. The result indicated that the CdS catalysts are fairly photostable and practically applicable. It was claimed that electron-donating functional groups of phytochemical present in aqueous extract of *C. gigantea* leaves are responsible for the stability of CdS NPs and the reduction of both dyes. Further, CdS NPs were evaluated for antimicrobial activity and compared with that exerted by core *C. gigantea* leaves extract. In the culture of bacteria, *E. coli*, *P. aeruginosa*, *S. aureus* and *B. thuringiensis*; and fungi, *A. niger* and *C. albicans*; zone of inhibition obtained with CdS NPs were 4 to 6 times wider than those obtained with *C. gigantea* leaves extract. About antifungal activity, it was claimed that CDs NPs got saturated and adhered to fungal hypha and to disrupt them.

### 2.6 Magnesium oxide nanoparticles

As such oral magnesium supplements are consumed to increase insulin sensitivity and reducing the risk of the onset of type 2 diabetes. This is because magnesium is an important co-factor/prosthetic group for phosphorylation causing enzymes like tyrosine-kinase, playing a significant role in insulin signalling pathway. But commonly available supplement, magnesium oxide, MgO has poor oral bioavailability and thereby may get decomposed by gastric acid. Hence, with the hypothesis that nanoencapsulated magnesium oxide nanoparticles (MgO NPs) can avoid all these biochemical degradation of MgO and increase its bioavailability. Carried out the synthesis of MgO NPs using aqueous extract of *C. gigantea* and their nano-encapsulation into polymer polyvinylpyrrolidone (PVP) or Eudragit L [30]. Aqueous extract of *C. gigantea* leaves played a significant role in the formation and stabilization of MgO NPs. The MgO NPs so formed were then encapsulated by following conventional emulsion solvent evaporation method where 10 mg of MgO NPs and 20 mg of PVP or 20 mg of Eudragit L were dissolved in 10 mL of ethanol. Then, about 10 mL of distilled water containing Tween80 (2%, w/w) or 10 mL liquid paraffin containing sorbitan sesquioleate (2%, w/w) was added as the emulsifier. Then, these mixtures

were heated to 80°C and stirred at an agitation speed of 250 rpm on a magnetic stirrer until ethanol was fully disappeared and that nanosuspensions were centrifuged at 13200 rpm for 20 mins to get PVP-MgO NPs or Eudragit L-MgO NPs. The average size of MgO NPs obtained was 48.38 nm while their crystallite size was 8 nm. When encapsulated by emulsion solvent evaporation, PVP-MgO NPs and Eudragit L-MgO NPs, particle size increased to 96.65 and 53.37 nm, respectively. Eudragit L-MgO NPs had higher stability. Drug entrapment efficiency (%) and drug loading (%) for Eudragit L-MgO NPs were found higher than those for PVP-MgO NPs. It was also observed that drug release pattern of Eudragit L-MgO nanoparticles was as per Fickian diffusion mechanism and coincided well with the Weibull model.

### 2.7 Nickel and nickel oxide nanoparticles

Nickel (Ni) is the transition metal, exhibiting magnetism and catalytic properties. Nickel nanoparticles (NiNPs) have been proved to adsorb environmentally hazardous dyes and inorganic pollutants [31]. They also possess good antibacterial and anti-inflammatory activities [32]. On the other hand, its oxide form NiO has cubic crystal lattice structure with p-type semiconductor properties. Nanoparticles of NiO (NiO-NPs), due to their electron transfer capability with their own high chemical stability and super-capacitance properties [33]; they exhibit technical applications in battery cathodes, fuel cells, electrochromic films, magnetic materials, optical fibres and gas sensors [34]. Considering these potential applications, Din et al. [35] fabricated Ni-NPs and NiO-NPs using hydro-methanolic (40% methanol) extract of freshly collected leaves of *C. gigantea*. In UV/vis spectrum, sharp exciton absorption was positioned at 415 nm, suggested that *C. gigantea* extract assisted green synthesised NiO NPs were stable. The FT-IR spectra of both Ni and NiO NPs did not show a peak around 1000–1100  $\text{cm}^{-1}$  while peak for O–H bond got reduced in Ni NPs FTIR spectrum and almost completely reduced in NiO NPs FTIR spectrum; suggesting the important role of alcohols and halogens in metal ion reduction. Amines also played role as a capping agent in the fabrication of Ni-NPs. As per the results of XRD-analysis the particle size of Ni-NPs was in the range of 20–40 nm while that may higher up to 60 nm for NiO NPs. Further, on antimicrobial screening of Ni and NiO-NPs against *Pseudomonas aeruginosa*, these were found equally potent, compared to Chloramphenicol.

### 2.8 Titanium dioxide nanoparticles

Infection by tick parasites like *Rhipicephalus microplus* and *Haemaphysalis bispinosa* is major hindrance in having and sustaining new generations of cattle. To have a scientific check for hypothesis that titanium dioxide nanoparticles (TiO<sub>2</sub> NPs) could be exhibiting significant

acaricidal activity, Marimuthu et al. [36] attempted the green synthesis of  $\text{TiO}_2$  NPs using aqueous extract *C. gigantea* flowers and morphologically characterised. XRD pattern of  $\text{TiO}_2$  NPs showed diffraction peaks at  $2\theta$  values of  $27.33^\circ$ ,  $35.83^\circ$ ,  $43.87^\circ$ ,  $54.02^\circ$ ,  $56.39^\circ$ ,  $66.64^\circ$  and  $74.07^\circ$  could be assigned to the (110), (101), (210), (211), (220), (301) and (320), respectively; indicating faced centre cubic lattice structure of  $\text{TiO}_2$  NPs. SEM showed their spherical shape with particle size ranging between 160 and 220 nm [36]. also evaluated  $\text{TiO}_2$  NPs against *R. microplus* and *H. bispinosa* by filter paper impregnated bioassay protocol. Researchers found that  $\text{LC}_{50}$  values shown by aqueous extract of flowers and  $\text{TiO}(\text{OH})_2$  solution are around four times higher than those shown by  $\text{TiO}_2$  NPs, indicating  $\text{TiO}_2$  NPs can be used to treat the tick parasitic infection in cattle.

### 2.9 Cupric oxide nanoparticles

To fulfil the increasing demands for energy, the development of photovoltaic technology especially, dye-sensitised solar cells (DSSCs) are getting importance and research interest. Cupric oxide ( $\text{CuO}$ ) is a p-type semiconductor with narrow bandgap (Eg 1.2 eV) and material for the fabrication of various electronic and optoelectronic devices [37]. Therefore, in the fabrication of DSSCs,  $\text{CuO}$  NPs have been considered as an alternative counter electrode material.  $\text{CuO}$  NPs can also be used in making high-temperature superconductors [38] gas sensors [39] and giant magnetoresistance materials [40]. When incorporated into coatings, plastics and textiles,

$\text{CuO}$  NPs acts as anti-fouling and antimicrobial [41]. Considering these technical applications, Sharma et al. [42], synthesised  $\text{CuO}$  NPs from Cupric Nitrate added to aqueous extract of *C. gigantea* leaves and fabricated  $\text{CuO}$  nanoparticles based counter electrode that to be used in DSSC. Initially, the formation of nanostructures was confirmed by the increased bandgap of 1.86 eV. In XRD analysis, several intense peaks at  $2\theta$  values of  $32.4^\circ$ ,  $35.5^\circ$ ,  $38.7^\circ$ ,  $48.7^\circ$ ,  $53.4^\circ$ ,  $58.3^\circ$ ,  $61.5^\circ$ ,  $66.2^\circ$ ,  $68.0^\circ$ ,  $72.4^\circ$  and  $75.2^\circ$ , were obtained, which could be assigned to (110), (002), (111), (202), (020), (202), (113), (311), (113), (311) and (222), respectively; indexing as typical monoclinic structure of  $\text{CuO}$  NPs. TEM analysis revealed the spherical shape of  $\text{CuO}$  NPs with a particle size up to 20 nm. The cyclovoltametric measurement exposed that  $\text{CuO}$  NPs-based material showed to be a reasonably good platform for the reduction of triiodide ions in redox electrolyte, signifying its good electrocatalytic activity towards the iodide ions (Fig. 2). Kumari et al. [43] attempted synthesis of  $\text{CuO}$  NPs by the addition of floral extract of *C. gigantea* to 1 mM  $\text{CuCl}_2$  solution and characterised by advanced techniques. The hydrodynamic diameter of synthesised  $\text{CuO}$  NPs showed the diameter of  $109 \pm 11$  nm. The zeta potential of  $\text{CuO}$  NPs was found to be  $-34 \pm 12$  mV. The XRD peaks were observed at  $2\theta$  values of  $32.5^\circ$ ,  $35.5^\circ$ ,  $38.7^\circ$ ,  $48.7^\circ$ ,  $53.0^\circ$ ,  $58.2^\circ$ ,  $63.4^\circ$ ,  $66.2^\circ$  and  $68.1^\circ$  corresponding to (110), (002), (111), (202), (020), (202), (113), (311) and (113), respectively. The result indicated a typical monoclinic structure of  $\text{CuO}$  NPs [43]. also explained the mechanism of

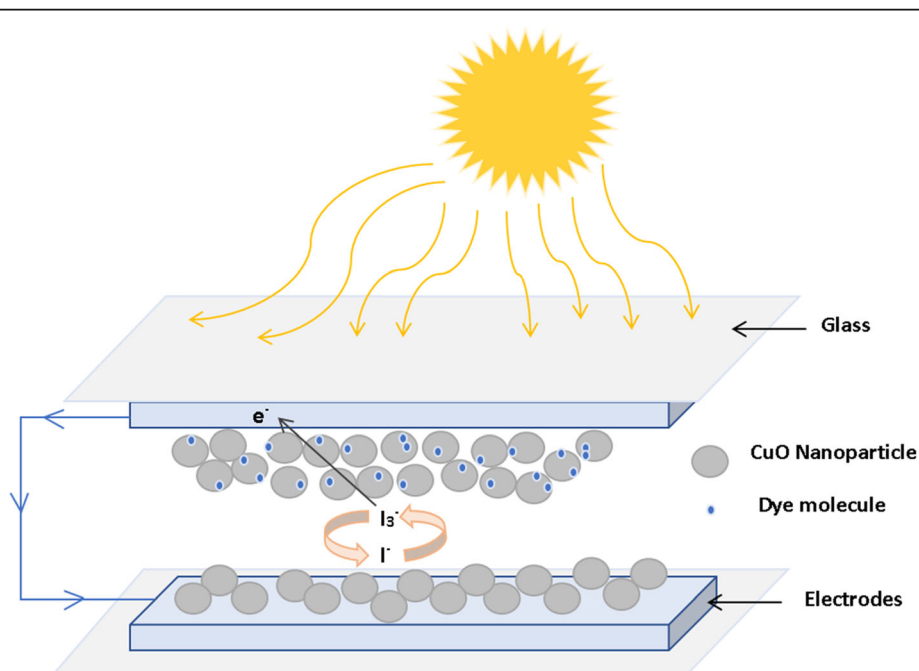
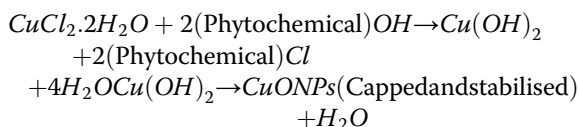


**Fig. 2** Cupric oxide nanoparticles ( $\text{CuO}$  NPs) employed in dye-sensitized solar cells (DSSCs)

biosynthesis of CuO NPs, according to which phytochemicals having hydroxyl groups played a significant role in reducing copper (II) chloride to copper hydroxide (Cu (OH)<sub>2</sub>). Further, Cu (OH)<sub>2</sub> got reduced to CuO NPs which were capped and stabilised by phytochemicals present in the floral extract of *C. gigantea* extracted in an aqueous medium.



The toxicity of CuO NPs was evaluated by determining their effect on physiological and morphological changes in Zebrafish embryo. Surprisingly, the hatching rate was found higher in the case of embryos exposed to CuO NPs as compared to the commercial one. It was also observed that CuO NPs got accumulated at chorion, yolk sac and skin surface of 24, 48 and 72 h post-fertilization (hpf).

To determine the effect of synthesised CuO NPs in Zebrafish embryos at the cellular level, ROS induction and apoptosis were analysed in embryos after 72 hpf of treatment with the help of flow cytometry and Acridine orange staining-based fluorescent microscopy.

### 2.10 Zinc oxide nanoparticles

Two successful attempts were made for green synthesis of zinc oxide nanoparticles (ZnO NPs) using *C. gigantea*. Vidya et al. [44] used aqueous extract of *C. gigantea* leaves. They got hexagonal ZnO NPs ranging in size of 30–35 nm. Panda et al. [45] employed milky latex obtained by making an incision on the intact branches of *C. gigantea* and precursor zinc acetate; and carried out alkaline precipitation method. XRD pattern showed 13 characteristic diffraction peaks of (100), (002), (101), (102), (110), (103), (200), (112), (201), (004), (202), (104) and (203), observed at 2θ angles; 31.77°, 34.42°, 36.25°, 47.54°, 56.6°, 62.86°, 66.38°, 67.96°, 69.09°, 72.56°, 76.95°, 81.37° and 89.6°, respectively, reflecting wurtzite crystalline structure of ZnO NPs. *C. gigantea* milky latex-based ZnO NPs induced oxidative stress in DNA damage as determined by Comet assay in the root assay system of *L. sativus*, which was found comparable to that induced by the commercially available ZnO NPs-S (S for Sigma-Aldrich, St. Louis, MO, USA).

### 2.11 Silver nanoparticles

Rajkuberan et al. [46] synthesised silver nanoparticles (AgNPs) using freshly collected milky white latex of *C. gigantea*. Latex was first converted to 3% aqueous extract and then about 1 ml was added to 9 ml of 2 mM silver nitrate, AgNO<sub>3</sub>. Then, AgNPs were characterised

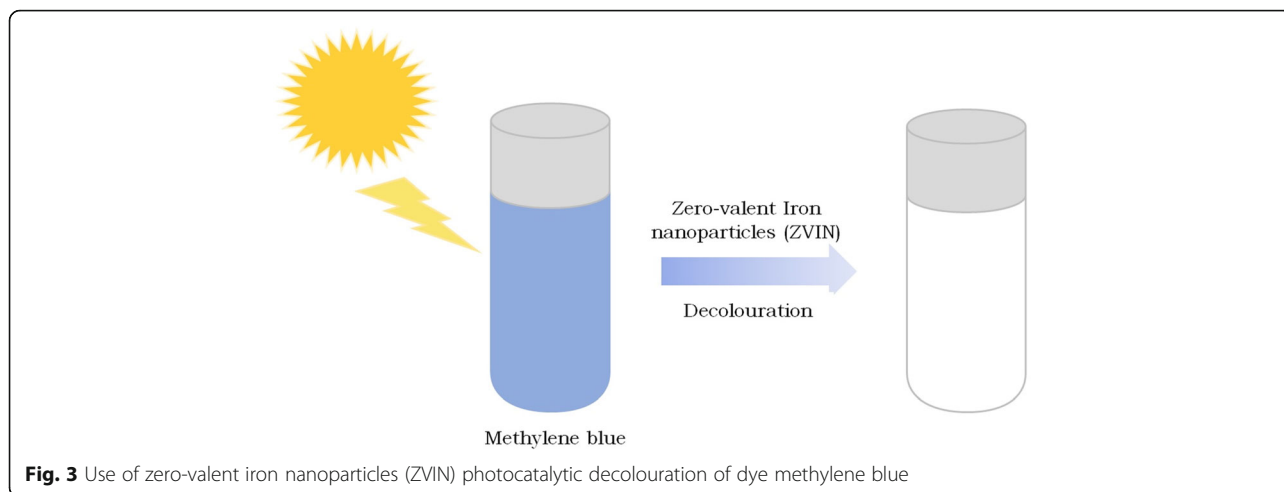
by UV-Vis absorbance spectroscopy, FTIR analysis, X-ray diffraction, FeSEM and TEM techniques; and evaluated for their antibacterial activity against *Shigella* and *P. aeruginosa*; and cytotoxicity against HeLa cells. XRD pattern showed diffraction peaks at (111), (101), (103) and (105) corresponded to 2θ values of 38.12, 47.08, 57.93 and 76.71°, respectively depicted that AgNPs had mixed phase of cubic and hexagonal structures. As per Debye–Scherrer's equation, the average particle size was calculated as 12 nm. About antimicrobial activity, it was observed that zone of inhibition created by lowest concentration 10 μl of AgNPs was 2 to 3 times higher in diameter than those created by 3% aqueous latex extract. Cytotoxicity exerted by these AgNPs against HeLa cells was also significant with LC<sub>50</sub> of 91.3 μg; however, that with 3% aqueous latex extract was found to be 311 μg.

### 2.12 Iron oxide nanoparticles and biomaterial-supported zero-valent iron nanoparticles

Jain et al. [47] employed aqueous extract of *C. gigantea* for phytofacation of iron oxide nanoparticles. The XRD pattern of the product can be clearly pointed to the face-centered cubic spine structure of iron oxide nanoparticles with a lattice parameter of  $a = 8.393 \text{ \AA}$  and a size ranging between 3 and 6 nm; exposing that reduction of Fe<sup>3+</sup> by *C. gigantea* aqueous extract leads to FeO NPs as the final product. Further, in 2018, zero-valent iron nanoparticles (ZVIN) were synthesised by green eco-friendly method using aqueous extract of *C. gigantea* flowers and characterised by UV-Vis, FT-IR, XRD, SEM, and EDX [48]. The ZVIN so synthesised were spherical in shape and 50–90 nm in size. From the FT-IR and UV-visible spectrum, Sravanthi et al. 2018 concluded that polyphenols present in the flower extract were responsible for the reduction and stabilization of ZVIN. Then, they proved the effectivity of ZVIN in controlling water pollution by adsorptive removal of organic waste such as methylene blue (synthetic dye) (Fig. 3) and aniline (aromatic primary amine) from contaminated water.

### 2.13 Tin oxide/stannic oxide nanoparticles

Tin oxide/stannic oxide (SnO<sub>2</sub>) is one of the n-type semiconductor having a bandgap of 3.6 eV, thereby used in photoconductive and photochemical device in liquid crystal display and lithium-ion batteries; and transparent conductive electrode for solar cells, gas sensors [49]. Because of the high surface to volume ratio, SnO<sub>2</sub> NPs exhibit increased sensitivity and adsorption and can be used as photocatalyst [50]. Considering this significance, Bhosale et. al. [51] attempted the green synthesis of SnO<sub>2</sub> NPs by the addition of dilute aqueous extract of leaves to 0.05 M solution of tin chloride (SnCl<sub>4</sub> · 5H<sub>2</sub>O) with constant stirring. They claimed that tin chloride reacted with polyphenols present in the extract and

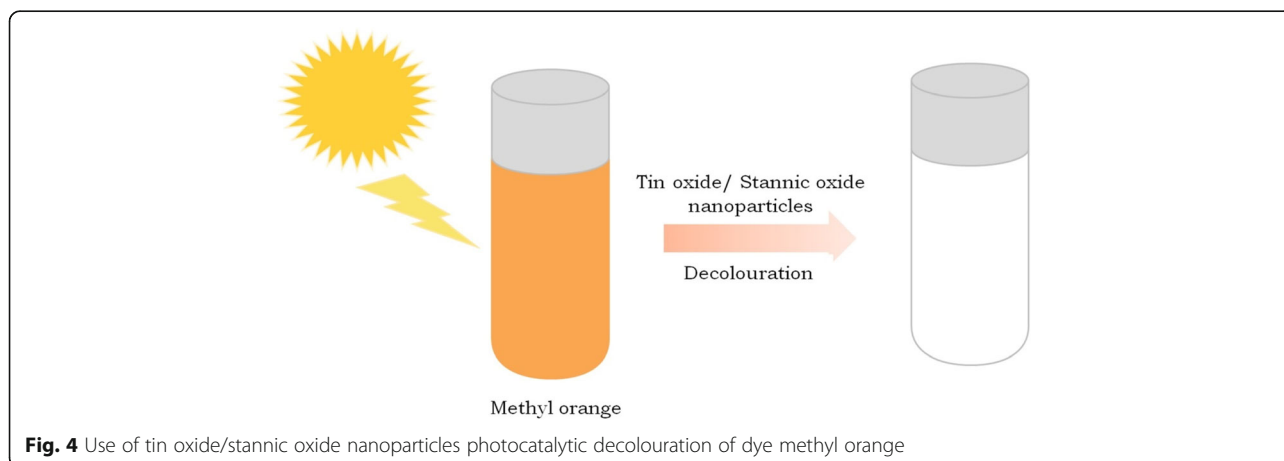


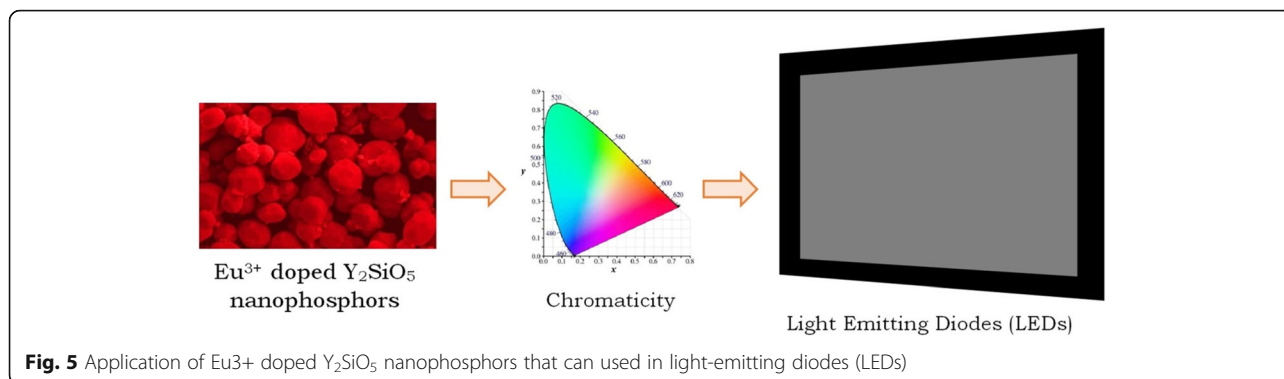
following calcination, they got  $\text{SnO}_2$  NPs with spherical morphology of an average size of 35 nm. In XRD pattern, the peaks at  $2\theta$  values of  $26.5^\circ$ ,  $34^\circ$ ,  $37.9^\circ$ ,  $51.7^\circ$ ,  $54.4^\circ$ ,  $57.7^\circ$ ,  $61.7^\circ$ ,  $64.8^\circ$ ,  $71.3^\circ$  and  $78.5^\circ$  were associated with (110), (101), (200), (211), (220), (002), (310), (301), (202) and (222) planes, respectively, proving the formation of  $\text{SnO}_2$  NPs with tetragonal structure. Then, Bho-sale et al. 2018 also explained the plausible mechanism for the formation of  $\text{SnO}_2$  NPs, according to which  $\text{SnCl}_4 \cdot 5\text{H}_2\text{O}$  salt solution on mixing with *C. gigantea* leaf extract,  $\text{Sn}^{4+}$  ions form a complex with hydroxyl groups. The complex so formed got decomposed on calcination. Polyphenolic molecules then kept  $\text{Sn}^{4+}$  cations together forming  $\text{SnO}_2$  NPs. Taking dye methyl orange as a model pollutant under UV-light, its degradation was further tested as a function of photocatalytic potential of the synthesised  $\text{SnO}_2$  NPs (Fig. 4).

#### 2.14 $\text{Eu}_3^+$ doped $\text{Y}_2\text{SiO}_5$ nanophosphors

During the last decade, white light-emitting diodes (WLEDs), due to high efficiency, energy-saving, long

lifetime, safety and environmental protection have fascinated a lot of research interest in the solid-state lighting [52]. White light was obtained by the foremost technique involving the mixing ultraviolet (UV) LED chip with tricolour phosphors [53] but the lack of appropriate red phosphors decreased colour rendering index (CRI). So far newly designed red phosphor,  $\text{Y}_2\text{O}_2\text{S}:\text{Eu}^{3+}$  has shown low efficiency and poor chemical stability. Therefore, Ramakrishna et al. [54] accepted this challenge of developing a new red phosphor with sufficiently high luminous efficiency and fabricated red-emitting  $\text{Eu}^{3+}$  doped  $\text{Y}_2\text{SiO}_5$  nanophosphors using *C. gigantea* latex, Yttrium nitrate ( $\text{Y}(\text{NO}_3)_3$ ), Europium nitrate ( $\text{Eu}(\text{NO}_3)_2$ ),  $\text{H}_2\text{O}$  and  $\text{NaCl}$ . The  $\text{Eu}^{3+}$  doped  $\text{Y}_2\text{SiO}_5$  nanophosphors so obtained were irregular shape with an average size of 32 nm which was found decreasing on the increasing concentration of ( $\text{Eu}(\text{NO}_3)_2$ ). Determination of optical properties of  $\text{Eu}^{3+}$  doped  $\text{Y}_2\text{SiO}_5$  nanophosphors was based on emission spectra and Judd–Ofelt theory. It was observed that there is ionic bonding between  $\text{Eu}^{3+}$  ions and host; and assembled in symmetrical in coordination





structure surrounding the (rare earth) RE ion. This newly synthesised phosphor exhibited admirable International Commission on Illumination (CIE) chromaticity coordinates (0.5866, 4026) and average correlated colour temperature CCT value 2018.5 K. Hence, researchers claimed that these Eu<sup>3+</sup> doped Y<sub>2</sub>SiO<sub>5</sub> nanophosphors could have potential application in the fabrication of near-ultraviolet excited white light-emitting diodes (Fig. 5).

### 3 Conclusion

*Calotropis gigantea* (Asclepiadeae) is the plant having several well-proved pharmacological actions. Several types of nanomaterials have been synthesised following green approach using aqueous extract of different parts of *C. gigantea*; evaluated for different pharmacological activities and potential were compared that with extracts. Nanomaterials tried to get synthesised include nanoparticles and nanophosphors. Importantly, green synthesis of nanoparticles has upsurge as new nanobiotechnology to produce eco-friendly and cost-effective synthetic processes for highly stable nanoparticles which emerges as a safer alternative to conventional methods. These nanoparticles were proved to have better antimicrobial action against both animal and plant infecting pathogens and utilities in controlling the water pollution by adsorbing or precipitating pollutants, demonstrated using dyes and other organic compounds. Nanophosphors have been extensively investigated during the last decade due to their application potential for various high-performance displays and devices.

#### Abbreviations

Ag NPs: Silver nanoparticles; CCT: Correlated colour temperature; CdS NPs: Cadmium sulphide nanoparticles; CRI: Colour rendering index; CuO NPs: Cupric oxide nanoparticles; FT-IR: Fourier transform-infrared spectroscopy; Ni-NPs: Nickel nanoparticles; NiO-NPs: Nickel oxide nanoparticles; SEM: Scanning electron microscopy; SnO<sub>2</sub> NPs: Tin oxide/stannic oxide nanoparticles; TEM: Transmission electron microscopy; TiO<sub>2</sub> NPs: Titanium dioxide nanoparticles; XRD: X-ray diffraction; ZnO NPs: Zinc oxide nanoparticles; ZVIN: Zero-valent iron nanoparticles

#### Acknowledgements

The author of this manuscript is thankful to Dr.(Mrs.) Anagha M. Joshi, Principal, SCES's Indira College of Pharmacy, Pune, for her encouragement

and also for providing internet and library facilities at the college premises to access the articles and books to carry out this review.

#### Author's contributions

SPP initiated the idea of designing this review, carried out the survey of the available literature and written the review manuscript. The author read and approved the final manuscript.

#### Authors' information

Mr. Shrinivas P. Patil has completed his M. Pharm with specialisation in Pharmacognosy in 2012. He has received Senior Research Fellowship for the project entitled, 'Quality standards of Indian Medicinal Plants and preparation of monographs thereon' sponsored by Indian Council of Medical Research, ICMR- New Delhi, India. He has several research articles pertaining to phytochemistry and pharmacology of medicinal plant to his credit. He has been recognised as reviewer for research articles to be published in International peer-reviewed journal groups. Currently, he is serving as Assistant Professor at SCES's Indira College of Pharmacy, Pune, affiliated to Savitribai Phule Pune University, SPPU (formerly University of Pune).

#### Funding

Not applicable

#### Availability of data and materials

Not applicable

#### Ethics approval and consent to participate

Not applicable

#### Consent for publication

Not applicable

#### Competing interests

The authors declare that they have no competing interests.

Received: 31 August 2019 Accepted: 15 January 2020

Published online: 01 April 2020

#### References

1. Antonietti M (2016) Small is beautiful: challenges and perspectives of nano/meso/microscience. *Small*. 12(16):2107–114
2. Na Y, Yang S, Lee S (2014) Evaluation of citrate-coated magnetic nanoparticles as draw solute for forward osmosis. *Desalination* 347:34–42
3. Davar F, Fereshteh Z, Salavati-Niasari M (2009) Nanoparticles Ni and NiO: synthesis, characterization and magnetic properties. *J Alloys Compd* 476(1–2):797–801
4. Kreyling WG, Semmler-Behnke M, Chaudhry Q (2010) A complementary definition of nanomaterial. *Nano Today* 5(3):165–168
5. Krishnamurthy N, Vallinayagam P, Madhavan D (2014) Engineering chemistry. PHI Learning Pvt Ltd, Delhi
6. Rahman MA, Wilcock CC (1991) A taxonomic revision of *Calotropis* (Asclepiadaceae). *Nord J Bot* 11(3):301–308



7. Lhinhatrakool T, Sutthivaiyakit S (2006) 19-nor- and 18, 20-epoxycardenolides from the leaves of *Calotropis gigantea*. *J Nat Prod* 69: 1249–1251
8. Seeka C, Sutthivaiyakit S (2010) Cytotoxic Cardenolides from the leaves of *Calotropis gigantea*. *Chem Pharm Bull* 58(5):725–728
9. Nguyen KDH, Dang PH, Nguyen HX, Nguyen MTT, Awale S, Nguyen NT (2017) Phytochemical and cytotoxic studies on the leaves of *Calotropis gigantea*. *Bioorg Med Chem Lett* 27:2902–2906
10. Habib MR, Karim MR (2009) Antimicrobial and cytotoxic activity of Di-(2-ethylhexyl) phthalate and anhydrosophoradiol-3-acetate isolated from *Calotropis gigantea* (Linn.) flower. *Mycobiology* 37(1):31–36
11. Sen S, Sahu NP, Mahato SB (1992) Flavonol glycosides from *Calotropis gigantea*. *Phytochemistry* 31(8):2919–2921
12. Lakshminarayana G, Rao KS, Pantulu AJ, Gupta DR (1988) Surface and Internal Lipids of *Calotropis gigantea* L. Leaves. *Fat Sci Technol* 90(Jahrgang Nr.2):65–67
13. Ali M.; Gupta J; Indian J. Chem., Sect. B: Org. Chem. Incl. Med. Chem. 38 (1999) 7, 877–881;
14. Kadiyal M, Ponnusankar S, Elango K (2013) *Calotropis gigantea* (L.) R. Br (Apocynaceae): a phytochemical and pharmacological review. *J Ethnopharmacol* 150(1):32–50
15. Pathak AK, Argal A (2007) Analgesic activity of *Calotropis gigantea* flower. *Fitoterapia* 78:40–42
16. Habib MR, Karim MR (2013) Effect of anhydrosophoradiol-3-acetate of *Calotropis gigantea* (Linn.) flower as antitumor agent against Ehrlich's ascites carcinoma in mice. *Pharmacol Rep* 65:761–767
17. Ishnava KB, Chauhan JB, Garg AA, Thakkar AM (2012) Antibacterial and phytochemical studies on *Calotropis gigantea* (L.) R. Br. Latex against selected cariogenic bacteria. *Saudi J Biol Sci* 19:87–91
18. Pattanaik PK, Dattatreya KD, Chhatroi H, Shahbazi S, Ghosh G, Kuanar A (2017) Chemometric profile & antimicrobial activities of leaf extract of *Calotropis procera* and *Calotropis gigantea*. *Nat Prod Res* 31(16):1954–1957
19. Chitme HR, Chandra R, Kaushik S (2005) Evaluation of antipyretic activity of *Calotropis gigantea* (Asclepiadaceae) in experimental animals. *Phytother Res* 19:454–456
20. Habib MR, Karim MR (2011) Evaluation of antitumor activity of *Calotropis gigantea* L. root bark against Ehrlich ascites carcinoma in Swiss albino mice. *Asian Pac J Trop Med* 4:786–790
21. Argal A, Pathak AK (2006) CNS activity of *Calotropis gigantea* roots. *J Ethnopharmacol* 106:142–145
22. Ghule SD, Vidyasagar G, Bhandari A, Sharma P, Gunjal AP (2014) CNS activity of leaves extract of *Calotropis gigantea*. *Asian Pac J Trop Dis* 4(Suppl 2): S902–S905
23. Taylor P, Arsenak M, Abad MJ, Fernández A, Milano B, Gonto R, Ruiz MC, Fraile S, Taylor S, Estrada O, Michelangeli F (2012) Screening of Venezuelan medicinal plant extracts for cytostatic and cytotoxic activity against tumor cell lines. *Phytother Res* 24(4):530–539
24. Wong SK, Lim YY, Abdullah NR, Nordin FJ (2011) Assessment of antiproliferative and antiplasmodial activities of five selected Apocynaceae species. *BMC Complement Altern Med* 11(3):1–8
25. Parhira S, Zhu G, Chen M, Bai L, Jiang Z (2016) Cardenolides from *Calotropis gigantea* as potent inhibitors of hypoxia-inducible factor-1 transcriptional activity. *J Ethnopharmacol* 194:930–936
26. Deshmukh PT, Fernandes J, Akarte A, Toppo E (2009) Wound healing activity of *Calotropis gigantea* root bark in rats. *J Ethnopharmacol* 125:178–181
27. Srivastava SR, Keshri G, Bhargavan B, Singh C, Singh MM (2007) Pregnancy interceptive activity of the roots of *Calotropis gigantea* Linn. In rats. *Contraception* 75:318–322
28. Rajesh R, Gowda CDR, Nataraju A, Dhananjaya BL, Kemparaju K, Vishwanath BS (2005) Procoagulant activity of *Calotropis gigantea* latex associated with fibrin (ogen)olytic activity. *Toxicol* 46:84–92
29. Ayodhya D, Veerabhadram G (2017) One-pot green synthesis, characterization, photocatalytic, sensing and antimicrobial studies of *Calotropis gigantea* leaf extract capped CdS NPs. *Mat Sci Engineering B* 225:33–44
30. Hii YS, Jaison Jeevanandam J, San Chan YS (2018) Plant mediated green synthesis and nanoencapsulation of MgO nanoparticle from *Calotropis gigantea*: Characterisation and kinetic release studies. *Inorg Nano-Met Chem* 48 (2018):620–31
31. Pandian CJ, Palanivel R, Dhananasekaran S (2015) Green synthesis of nickel nanoparticles using *Ocimum sanctum* and their application in dye and pollutant adsorption. *Chin J Chem Eng* 23(8):1307–1315
32. Angajala G, Radhakrishnan S (2014) A review on nickel nanoparticles as effective therapeutic agents for inflammation. *Inflamm Cell Signal* 1(3):1–8
33. Thema F, Manikandan E, Gurib-Fakim A, Maaza M (2016) Single phase Bunsenite NiO nanoparticles green synthesis by *Agathosma betulina* natural extract. *J Alloys Compd* 657:655–661
34. Borgström M, Blart E, Boschloo G, Mukhtar E, Hagfeldt A, Hammarström L, Odobel F (2005) Sensitized hole injection of phosphorus porphyrin into NiO: toward new photovoltaic devices. *J Phys Chem B* 109(48):22928–34
35. Din MI, Nabi AG, Rani A, Aihetasham A, Mukhtar M (2018) Single step green synthesis of stable nickel and nickel oxide nanoparticles from *Calotropis gigantea*: catalytic and antimicrobial potentials. *Environ Nanotechnol Monit Manag* 9:29–36
36. Marimuthu S, Rahuman AA, Jayaseelan C, Kirithi AV (2013) Acaricidal activity of synthesized titanium dioxide nanoparticles using *Calotropis gigantea* against *Rhipicephalus microplus* and *Haemaphysalis bispinosa*. *Asian Pac J Trop Med* 6:682–688
37. Kumar RV, Elgamiel R, Diamant Y, Gedanken A, Norwig J (2001) *Langmuir* 17:1406–1410
38. Malandrino G, Condorelli GG, Lanza G, Fragala IL, Alloys J (1997) *Compd* 251:314–316
39. Ishihara T, Higuchi M, Takagi T, Ito M, Nishiguchi H, Takita T (1998) *J Mater Chem* 8:2037–2042
40. Liu X, Bi N, Feng C, Or SW, Sun Y, Jin C, Li W, Xiao F, Alloys J (2014) *Comp* 587:1–5
41. Apostolov AT, Apostolova IN, Wesselinowa JM (2014) *Solid State Commun* 192:71–74
42. Sharma JK, Akhtar MS, Ameen S, Srivastava P, Singh G (2015) Green synthesis of CuO nanoparticles with leaf extract of *Calotropis gigantea* and its dye-sensitized solar cells applications. *J Alloys Compd* 632:321–325
43. Kumari P, Panda PK, Jha E, Kumari K, Nisha K, Mallick MA, Verma SK (2017) Mechanistic insight to ROS and Apoptosis regulated cytotoxicity inferred by green synthesized CuO nanoparticles from *Calotropis gigantea* to embryonic Zebrafish. *Sci Rep* 7:16284
44. Vidya C, Hiremath S, Chandraprabha MN, Antonyraj MAL, Venu GI, Jain A, Kokil BK (2013) Green synthesis of ZnO nanoparticles by *Calotropis gigantea*. *Int J Curr Engineering Technol* (1):118–20
45. Panda KK, Golar D, Venugopal A, Achary VMM, Phaomei G, Parinandi NL, Sahu HK, Panda BB (2017) Green synthesized zinc oxide (ZnO) nanoparticles induce oxidative stress and DNA damage in *Lathyrus sativus* L. Root Bioassay System. *Antioxidants* 6:35
46. Rajkuberan C, Sudha K, Sathishkumar G, Sivaramakrishnan S (2014) Antibacterial and cytotoxic potential of silver nanoparticles synthesized using latex of *Calotropis gigantea* L. *Spectrochimica Acta Part A: Mol Biomol Spectroscopy* 136B:924–30
47. Jain D, Rathore KS, Jain R, Singh H, Kachhwaha S, Kothari SL (2013) Phytofabrication of Iron oxide nanoparticles using *Calotropis gigantea* L. *Adv Sci Focus* 4(1):318–321
48. Sravanthi K, Ayodhya D, Swamy PY (2018) Green synthesis, characterization of biomaterial-supported zero-valent iron nanoparticles for contaminated water treatment. *J Analytical Sci Technol* 9:3
49. Naje AN, Norry AS, Suhail AM (2013) *IJRSET* 2:7068
50. Suwarnkar MB, Kadam AN, Khade GV, Gavade NL, Garadkar KM (2016) *J Mater Sci Mater Electron* 27:843
51. Bhosale TT, Shinde HM, Gavade NL, Babar SB, Gawade VV, Sabale SR, Kamble RJ, Shirke BS, Garadkar KM (2018) Biosynthesis of SnO<sub>2</sub> nanoparticles by aqueous leaf extract of *Calotropis gigantea* for photocatalytic applications. *J Mater Sci*. volume 8
52. Yu R, Noh H, Moon B, Choi B, Jeong, Lee H, Jang K, Yi S (2014) *J Lumin* 145: 717–722
53. Liang CH, Chang YC, Chang YS (2008) *Appl Phys Lett* 93:211902
54. Ramakrishna G, Nagabhushana H, Daruka PD, Vidya YS, Sharma SC, Anantharaju KS, Prashantha SC, Choudhary N (2016) Spectroscopic properties of red emitting Eu<sup>3+</sup> doped Y<sub>2</sub>SiO<sub>5</sub> nanophosphors for WLED's on the basis of Judd-Oftelt analysis: *Calotropis gigantea* latex mediated synthesis. *J Lumin* 181:153–63

## Publisher's Note

Springer Nature remains neutral with regard to jurisdictional claims in published maps and institutional affiliations.